SPE/DOE/GRI

Society of Petroleum Engineers | Dept. of Energy | Gas Research Institute

SPE/DOE/GRI 12860

Stress Ratio and Stress Trajectory Simulations for Devonian Gas Shales

by S.H. Advani, *Ohio State U.;* Anthony Andrews, *Battelle Laboratories;* J.K. Lee, *Ohio State U.;* and C.A. Komar,* *U.S. DOE*

*Member SPE-AIME

ABSTRACT

A brief review of selected in situ stress studies is presented. Pertinent geomechanical factors and rationale for stress trajectory characterizations are discussed in the context of natural fracturing in geological formations. Examples with structural cross sections incorporating the influence of the Rome Trough are identified and potential mechanisms for in situ stress reorientation and tectonic relief across selected regions in the Appalachian Plateau Province in West Virginia are given. Detailed finite element stress simulations and stress ratios associated with cross sections through Southeastern Kanawha County extending from the Warfield anticline to the Cabin Creek syncline are also reported. A discussion of these results and their correlation with available data and salient structural features is also given. In addition, the role of stress ratios, using a compressive-shear failure criterion, is emphasized in relation to the natural fracture systems in the Devonian shales.

INTRODUCTION

The phenomenological theories of gas production, from a rock mechanics vantage point, are related to the inherent characteristics of the natural fracture system and their subsequent linking with induced fracturing. A detailed knowledge of the prevalent reservoir in situ stress fields and gradients can provide fundamental data regarding preferential orientations, governing mechanisms, and optimum design of stimulation treatments [1,2]. Several stress mediated mechanisms that generate endogeneous and exogeneous fractures have been postulated in the literature [3,4]. A presentation of basic concepts for the analysis of fracture and fault development has been given by Bombolakis [5]. Considerable research has also been conducted on various methods for mapping fractures/joints, surface measurements, directional physical property measurement of oriented cores, mini-hydraulic fracture tests and their correlation with in situ stress magnitudes and orientations [6,7,8,9]. A comprehensive compilation of pertinent work related to the Eastern Gas Shales Project has been recently conducted by Cliffs Minerals [10]. Representative relationships between structure and stress ratio were developed at the Morgantown Energy Technology Center with a modified form presented in Reference [10]. Based on a study by Lewin and Associates, Inc., the stress ratio index appears to serve as a valid indicator for fracture spacing [11].

A study on the influence of burial history on subsurface horizontal stress variation formations with different mechanical properties has been reported by Prats [12]. This work demonstrates the effects of creep, temperature, material property and strain alterations during burial on the current stress state. A related investigation, using laboratory determined material properties, correlates field measured horizontal stress data with overburden induced stresses associated with the slope of the confining stress-axial stress curve and vertical temperature gradients [13]. Use of this in situ stress data base for granite, sandstone, limestone shale, and salt as a tool for optimizing fracture containment design has been advanced by Voegele et al. [14]. The in situ stress difference ($\sigma_{OVERBURDEN}-\sigma_{HMIN}$) versus σ_{HMIN} plots can be re-interpreted in terms of stress ratios and are more realistic indicators than Poisson ratio deduced values. An evaluation of the effect of Poisson's ratio on various rock material properties has been conducted by Kumar [15].

In this paper, previous modeling work [16,17] on stress trajectory characterizations across the Appalachian Plateau Province in West Virginia is used as a basis for studying, in site specific detail, the influence of the Rome Trough and mechanisms for in situ stress relaxation. Results from sample stress trajectory simulations of cross sections through Southeastern Kanawha County, West Virginia from the Warfield anticline to the Cabin Creek syncline are reported. A discussion of these results and their correlation with available data and key geomechanical features is presented. Also, the dominant role of the stress ratio, using a compressive-shear failure criterion with Devonian shale internal friction and ultimate compressive strength properties is demonstrated, in relation to natural fracturing. Finally,

References and illustrations at end of paper.

other generic applications of the developed methodology are identified.

GEOMECHANICAL MODEL DEVELOPMENT

Feasibility studies on stress trajectory simulations for model representations of selected regions overlying the Rome Trough, a buried rift system in the Appalachian basin, have been previously investigated [16,17]. Geological structures within the Appalachian basin were modeled by rigid basement structures containing potentially active faults overlain by passive sedimentary cover with potential slip zones along bedding planes. The basement faults formed the boundaries of the sedimentary cover and the depths of this cover were considerably smaller than the modeled horizontal distances (plane strain model). This work demonstrated the stress relieving effects of buttress and slip mechanisms and the applicability of the finite element approach as a tool for the analysis of in situ stresses in reservoir stratigraphic formations with defined boundary conditions, material property data, layered media descriptions, and interface conditions. The computed stress ratios can provide diagnostic information on the magnitude of tectonic relief, the extent of fracturing in gas producing zones, and choice of optimum stimulation treatments. The cited geomechanical studies demonstrate that the maximum horizontal stresses over the Rome Trough parallel the trend of the rift system and are related to the basement faulting. Also, the presence of tectonically relaxed zones, obtained for several basement interaction phenomenological models, suggests that the subsurface Rome trough influences the modern state of stress in the target pay zones (e.g. Brown and Black Devonian shales).

Based on the aforementioned studies, the region selected for the development of a detailed geomechanical model is the Cabin Creek district in Kanawha County, West Virginia. Occupying an area of 235 square miles, it is located South and Southeast of Louder, Malden, and Elk district in the Southeastern portion of the county. Good gas production has been found above the Devonian in the Big Line and Weir Sand. Near the surface, Cabin Creek has two distinguishing structural features; the Warfield anticline to the Northwest and the Wake Forest anticline to the Southeast. These anticlines were selected as bounds for the geomechanical model cross-section locations defined in Fig. 1. Analyses of these four cross sections have been conducted by Andrews [18] based on isopach and structural contours, and seismic data provided by Kulander [19]. Figure 2 illustrates details of a representative cross-section (#1) with the Cambrian clastic and carbonate units thickening appreciably in the Rome trough. A key to this cross section is provided in Table I. Cross section #1 is characterized by three important geologic features:

(i) A uniformity in orientation of the corresponding horizontal stress trajectory
(ii) division of a coal fracture domain boundary and
(iii) eastern flank of the Rome trough.

The approach to conducting the model simulations for this investigation considered the application of boundary tectonic loads based on in situ stress measurements and parameter sensitivities associated with material property variations and boundary conditions. Gravitational load models with horizontal confinement were initially studied followed by various tectonic load simulation models to represent different end conditions and the influence of a decollement surface in the Upper Silurian. The initially selected material property values corresponding to the finite element discretized strata presented in Fig. 3 are provided in Table II.

GEOMECHANICAL MODEL SIMULATIONS AND RESULTS

The model simulations were conducted using an in-house developed finite element program for geomechanical problems. The basic gravity load model entailed use of the initial property values from Table II, roller supports at the Northwest (NW) and Southeast (SE) ends, and complete displacement confinement at the basement as shown in Fig. 4a. The computed stress ratios in the Devonian shale for this benchmark case are also shown in this figure with the principal stress fields illustrated in Fig. 4b. It should be noted that tension zones are evident in selected Devonian shale regions, in the absence of external horizontal tectonic activity. Additional simulations of this baseline model were also conducted to parametrically examine the influence of elastic modulus reduction and Poisson ratio variation [18]. No significant parametric sensitivity trends were identified.

The subsequent tectonic load models were conducted to examine sensitivities to various end loading conditions, material property values, and layer interface conditions. As revealed in Fig. 5 and the accompanying Table III, the stress ratio (K) decreases dramatically from the SE to NW with the minimum horizontal stress related to the thrust faulting in the Valley and Ridge Province from the east. The depth to which this tectonic influence exists is uncertain. However, the existence of a decollement surface in the Upper Silurian was interpreted to indicate that the tectonic load extended to Unit 6. Below Unit 6, the effect of the tectonic load on the Devonian shale (Unit 6) is assumed to be insignificant with gravitational effects dominating. Two different approaches were utilized for the tectonic load model simulations. Firstly, tectonic loads were specified at both the NW and SE extremities and the resultant stress ratios and trajectories were obtained. Secondly, an attempt to force a stress ratio of K=0.7 at the NW end was made by varying the material properties, tectonic loading at the SE boundary and layer interface conditions.

Figures 6a and b reveal the computed Devonian shale stress ratios and principal stresses, respectively for the indicated loading with prescribed stress ratios of 0.7 at the NW and 1.0 at the SE. A uniform value of ν=0.25 and E reduced 25% below Unit 4 revealed minor changes in the principal stress magnitudes [18]. Significant tectonic relief is evidenced in the Devonian shale corresponding to the column elements 25 through 34 for all these simulated cases. As a follow-on to these studies, the stress response of the selected cross-section under a combination of gravitational and tectonic loading from the Southeast (K=1) was studied, using the initial material properties, with the Northwest end constrained as shown (Fig. 7a). Using this loading with a 90% reduced elastic modulus in Unit 6 (to simulate the decollement interface) and Poisson's ratio ν=0.30 in Units 3 through 5, the results are revealed in Fig. 7b. Extensive fracturing occurs in Devonian column elements 30 through 32 using the compression-shear failure criterion presented in the next section. Results using an interface joint element with different stiffness values between Units 5 and 6 yielded inconclusive results, although similar stress relaxation mechanisms were revealed. The final set of model simulations involved the use of a different stress ratio (K=2) at the Southeast end. The change in boundary stress ratio from K=1 to K=2 resulted in significant stress ratio changes only in the vicinity of the applied Southeast loading. This result suggests that the basement influenced stress responses mask the effects of applied horizontal tectonic loading from the Southeast. The effects of uniform tectonic stress imposed from the surface superposed with gravitational loading effects can also be similarly studied.

DISCUSSION AND CONCLUSIONS

Prior to a discussion of the results, it is desirable to present rock failure criteria in terms of the prevailing stress ratio, overburden stress, and material properties.

The compressive-shear failure criterion for rock is defined by

$$C_o = \sigma_1-\sigma_3[(\mu_f^2+1)^{1/2}+\mu_f]/[(\mu_f^2+1)^{1/2}-\mu_f] \qquad (1)$$

where, for our applications, σ_1 is the overburden stress (largest compressive stress), σ_3 is the minimum horizontal stress, C_o is the axial compressive strength of the rock, and μ_f is the surface fracture coefficient of friction. The angle at which fracture initiation will occur is defined by $\theta=0.5\tan^{-1}(1/\mu_f)$ and is measured from the axis of the overburden stress. Crack propagation with this loading will be a curved path (crack kinking) out of the plane of the pre-existing crack and will be governed by the prevailing principal stresses [20].

In addition to Eq.(1), Griffith shear and tensile fracture criteria can also be specified. However, the case represented above is most relevant to these investigations. Eq.(1) can be rewritten in the form

$$\sigma_1 = C_o/[1-K((\mu_f^2+1)^{1/2}+\mu_f)/((\mu_f^2+1)^{1/2}-\mu_f] \qquad (2)$$

where the stress ratio $K = \sigma_3/\sigma_1$. Table IV yields the computed compressive strengths required for rock failure with specified values of overburden stress, stress ratio, and coefficient of friction. Corresponding Mohr's circle plots and failure thresholds for Devonian shale have been presented by Andrews [18]. Eq.(2) can serve as a diagnostic indicator of the inherent natural fracture potential of a formation, as illustrated in Fig. 7b. As previously noted, the gravitational loading model merely provides calibrative stress response data relative to the selected material properties. The tectonic model with stress boundary conditions prescribed at both ends simulates an artificially isolated structure. However, this model furnishes sound mechanistic information pertinent to a reduced stress ratio over the abutment. The tectonic model, including decollement effects, with loading applied at the Southeast and normal displacement constraint at the Northwest boundary seemingly represents a physically more realistic case. A parametric sensitivity study for this model demonstrated that with a highly reduced modulus in Unit 6 and lumped Poisson's ratio of 0.35 in Units 3 through 5, a stress ratio of 0.70 in the Northwest can be approached.

The preceding simulations serve to illustrate the facilitating characteristics of the finite element model in predicting governing stress mediated mechanisms and in situ stress trajectories for layered geological formulations. The applicability of this methodology for gross in situ stress predictions for large scale cross-sections cannot yet be demonstrated because of the complexities associated with evaluation, stress history and boundary/interface conditions. Towse [21] has discussed these factors for low permeability upper cretaceous gas reservoirs in the Rocky Mountains by considering the rock properties and associated structures. The development of various faults (normal, overthrust, strike-slip) and reservoir fracture pattern correlations, from the vantage point of estimated in situ stress fields, has also been presented. Similar analysis, employing coupled local and gross finite element evaluations, will be very fruitful in defining joint/fracture orientations and extent. Finally, the presented techniques in conjunction with limited in situ stress field data, can be used for the preliminary stress analysis of mineback field sites, oil/gas reservoirs, and coal beds.

NOMENCLATURE

C_o	Uniaxial compressive strength
E	Elastic modulus
$K=\sigma_3/\sigma_1$	Stress ratio
σ_1	Effective overburden stress
$\bar{\sigma}_3$	Effective minimum horizontal stress
μ_f	Coefficient of friction
ν	Poisson's ratio

ACKNOWLEDGEMENTS

This research was sponsored by the U.S. Department of Energy under Contract DE-AC21-83-MC20338. Computational facilities were provided by IRCC at The Ohio State University.

REFERENCES

1. Komar, C.A., "Development of a Rationale for Stimulation Design in the Shale," Society of Petroleum Engineers of AIME, Paper No. SPE 7166, 1978.

2. Advani, S.H. et al., "The Role of Rock Mechanics in Optimizing Devonian Gas Production from the Appalachian Basin," Society of Petroleum Engineers of AIME, Paper No. SPE 10370, 1981.

3. Overbey, Jr., W.K., "Effect of In Situ Stress on Induced Fractures," Proceedings of the 7th Annual Appalachian Petroleum Geology Symposium, MERC/SP-72/2, 1976.

4. Badgley, P.C., "Structural and Tectonic Principles," Harper and Row, New York, 1965.

5. Bombolakis, E.G., "Some Constraints and Aids for Analysis of Fracture and Fault Development," Proceedings 2nd International Conference on New Basement Tectonics, 1976.

6. Overbey, Jr., W.K. and Rough, R.L., "Surface Studies Predict Orientation of Induced Formation Fractures," Producers Monthly, 32, 6, 1968.

7. Brechtel, C.E. et al., "In Situ Stress Determination in the Devonian Shales (Ira McCoy 20402) Within the Rome Trough Basin," Terra Tek Report TR-77-36, 1977.

8. Fairhurst, C., "Methods of Determining In Situ Rock Stresses at Great Depths," School of Mineral and Metallurgical Engineering Report, University of Minnesota, December 1967.

9. Blanton, T.L. et al., "Mechanical Properties of Devonian Shales from the Appalachian Basin," Science Applications, Inc. Final Report, Contract No. DE-AM21-78MC08216, 1981.

10. Anon, "Analysis of the Devonian Shales in the Appalachian Basin," Vol. I, Cliff Minerals Inc. Final Report, Contract No. DE-AC21-80MC-14693, September 1982.

11. Anon, "Analysis of Devonian Shale Gas Production Mechanisms in Application to Devonian Gas Shales of Ohio," Lewin and Associates, Inc. and Consultants Final Report, Contract No. DE-AC21-82MC-19239, January 1983.

12. Prats, M., "Effect of Burial History on the Subsurface Horizontal Stresses of Formations Having Different Material Properties," Society of Petroleum Engineers Journal, 658, December 1981.

13. Abou-Sayed, A.S., "Laboratory Evaluation of In-Situ Stress Contrast in Deeply Buried Sediments," Society of Petroleum Engineers of AIME, Paper No. SPE 11069, 1982.

14. Voegele, M.D. et al., "Optimization of Stimulation Design Through the Use of In-Situ Stress Determination," Journal of Petroleum Technology, 1071, June 1983.

15. Kumar, J., "The Effect of Poisson's Ratio on Rock Properties," Society of Petroleum Engineers of AIME, Paper No. SPE 6094, 1976.

16. Advani, S.H. et al., "Stress Trajectory Simulations Across the Appalachian Plateau Province in West Virginia," Proceedings First Annual Shale Symposium, pp. 320-327, 1977.

17. Chang, H.Y. et al., "Feasibility Study on Modeling of Stress Trajectories Across the Appalachian Plateau Province in West Virginia," Final Report West Virginia University, Contract No. EY-77-X-21-0368, 1978.

18. Andrews, A., "Stress Simulation Models in the Devonian Shales of Kanawha County, West Virginia: The Factors Influencing Fracturing with Respect to Natural Gas Production," M.S. Thesis, The Ohio State University, 1984.

19. Kulander, B., Wright State University, Personal Communications, 1983.

20. Nemat-Nasser, S. and Horii, H., "Compression-Induced Nonplanar Crack Extension with Application to Splitting, Exfoliation, and Rockburst," Journal of Geophysical Research 87, 6805, 1982.

21. Towse, D., "The Evolution and Stress History of the Low-Permeability Upper Cretaceous Gas Reservoirs in the Rocky Mountains," Lawrence Livermore Laboratory UCRL Preprint 83514, 1980.

PERIOD	SERIES	UNIT #	PREDOMINANT ROCK TYPE
PERMIAN PENNSYLVANIAN	Dunkard Series (ss & sh) Monongahelia Series (ss & sh) Conemaugh Series (ss & sh) Allegheny Series (ss) Pottsville Series (ss)	1	SANDSTONE
MISSISSIPPIAN	Mauch Chunk Series (sh) Greenbrier Series (lm)	2	SHALE
	Pocono Series Weir Sands Berea Sandstone	3	SANDSTONE
DEVONIAN	Devonian Shale Huron Member Java Formation West Falls Formation Sonyea Formation Genesse Formation	4	SHALE
SILURIAN	Onondaga (Huntersville) Chert Oriskany (Ridgeley) Sandstone Helderberg Formation (lm) Cayugan Series (ss/lm/dl/an) Williamsport Niagaran Series McKenzie Fromation (dl)	5	LIMESTONE
	Keefer Sandstone Rose Hill Formation (sh) Medinan Series Tuscarora Sandstone	6	SANDSTONE
ORDOVICIAN	Upper Ordovician Juniata Formation Martinsburg Shale	7	SHALE
	Middle Ordovician Chazy Chambersburg	8	LIMESTONE
	Lower Ordovician Conococheague, Stonehenge & Beekmantown	9	DOLOMITE
CAMBRIAN	Elbrook	10	LIMESTONE
	Rome (Waynesboro)	11	SHALE/ LIMESTONE
	Shady (Tomstown)	12	DOLOMITE
	Unicoi, Harpers & Antietam	13	SANDSTONE
PRECAMBRIAN			BASEMENT

TABLE I Key to Cross Sections

TABLE II
Selected Initial Material Properties

Unit	Rock Type	Specific Weight (lbs/cf)	Elastic Modulus (10x6 psi)	Poisson's Ratio
1	Sandstone	141.71	2.069	.25
2	Shale	171.05	5.0	.21
3	Sandstone	142.96	2.069	.38
4	Shale	162.84	4.4	.21
5	Limestone	171.0	12.0	.30
6	Sandstone	152.0	7.0	.25
7	Shale	166.0	5.0	.21
8	Limestone	172.0	12.0	.30
9	Dolomite	174.0	13.5	.34
10	Limestone	172.0	12.0	.30
11	Shale	166.0	5.0	.21
12	Dolomite	174.0	13.5	.34
13	Sandstone	168.0	7.0	.25

TABLE III
REFERENCES TO IN SITU STRESS MEASURMENTS

Plate Ref.	Hmax (psi)	Azmith	Hmin (psi)	Depth (feet)	V (psi)	Stress Ratio	Reference
1	5901	N50E 5	2610	2755	3036	.86	Haimson 1977 Devonian Shale
2	4390	N50E 5	2360	2745	3210	.73	Terra Tek 1977 Devonian Shale
3	3332	N50E 5	2374	2746	3095	.77	Lindner & Halprin 1978 Devonian Shale
4	-	-	-	-	-	-	Cliffs Minerals 1982
5	2305	N52W	1677	1100	1240	1.35*	Tosco/Agapito 1980 Coal
6	3172	N75E	1890	1100	1240	1.52*	Tosco/Agapito 1980 Coal
7	3380	N68E	2459	863	973	2.53*	Tosco/Agapito 1980 Coal
8	3339	N59E	2515	830	935	2.69*	Tosco/Agapito 1980 Coal
9	3815	N57E	3101	1140	1285	2.41*	Tosco/Agapito 1980 Coal
10	-	-	-	-	-	-	Cliffs Minerals 1982
11	-	-	-	-	-	-	Cliffs Minerals 1982
12	-	-	-	-	-	-	Cliffs Minerals 1982

* Calculated based on avg. sp. weight = 162 lbs/cf

TABLE IV Computed Shale Compressive Strengths for Specified σ_1, K, and $\mu_f = \tan\phi$

σ_1 = 5500 psi
Middle of Devonian Shale

ϕ	K = .2	.3	.4	.5
15°	3632	2698	1764	829
20°	3256	2134	1012	-
30°	2200	550	-	
40°	442	-		

σ_1 = 7000 psi
Bottom of Devonian Shale

ϕ	K = .2	.3	.4	.5
15°	4622	3433	2244	1055
20°	4145	2717	1289	-
30°	2800	700	-	
40°	561	-		

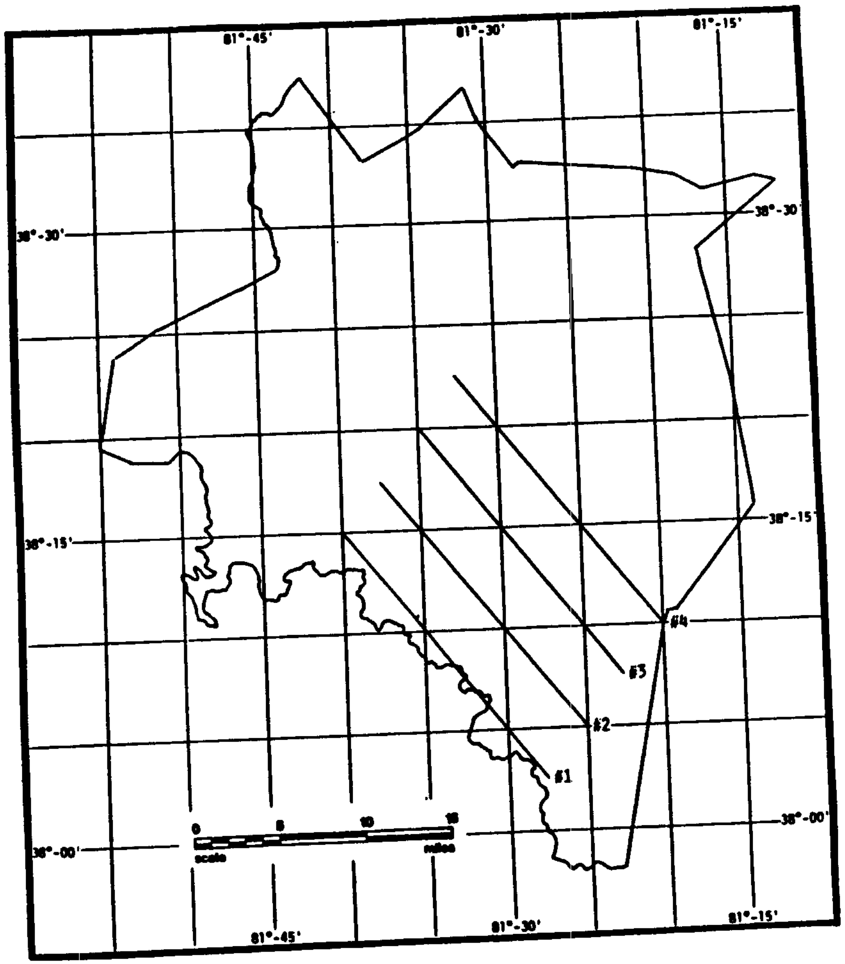

#1 - N38-15-00,W-40-00 to N38-02-30,W81-27-30
#2 - N38-17-30,W-37-30 to N38-05-00,W81-25-00
#3 - N38-20-00,W-35-00 to N38-07-30,W81-22-30
#4 - N38-22-30,W-32-30 to N38-10-00,W81-20-00

Fig. 1—Map of Kanawha County, WV, with cross-section locations.

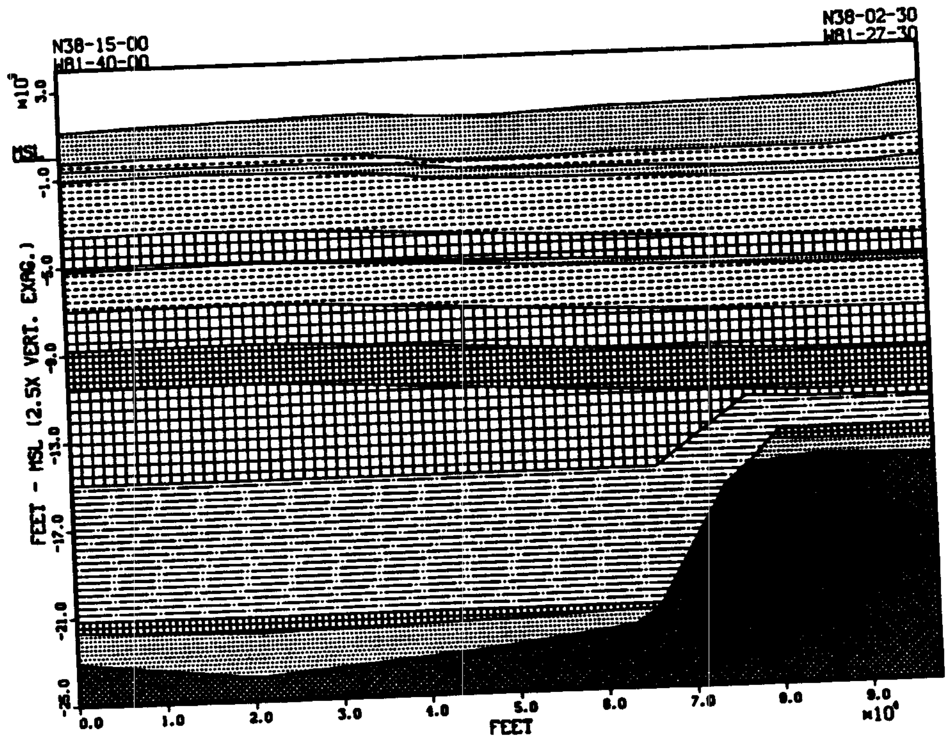

Fig. 2—Cross section No. 1, Cabin Creek field, Kanawha County, WV.

SPE 12286

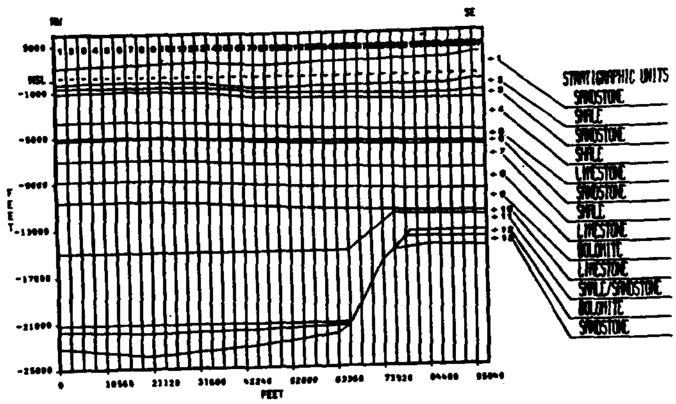

Fig. 3—Key to Cabin Creek field cross section.

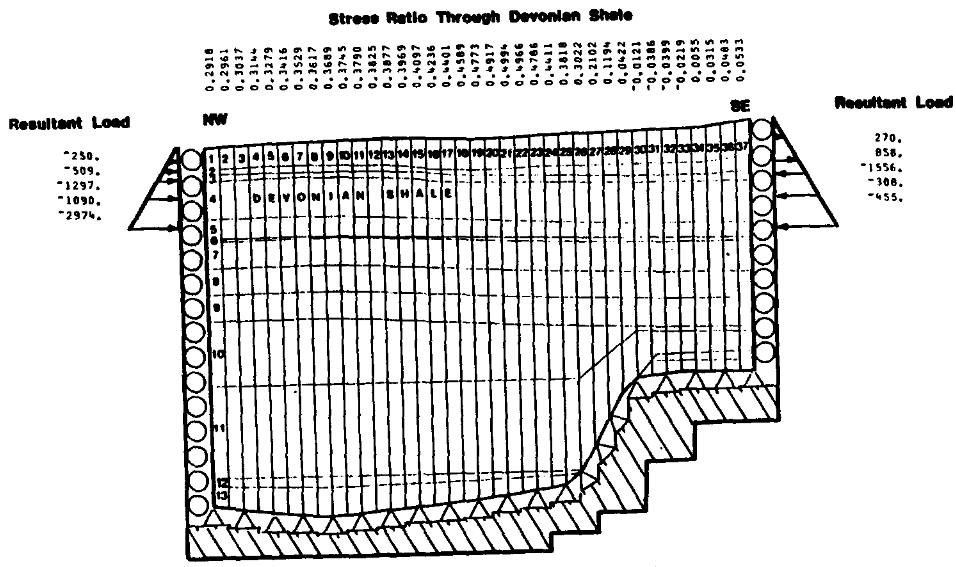

Fig. 4a—Gravitational load model with NW and SE confinement.

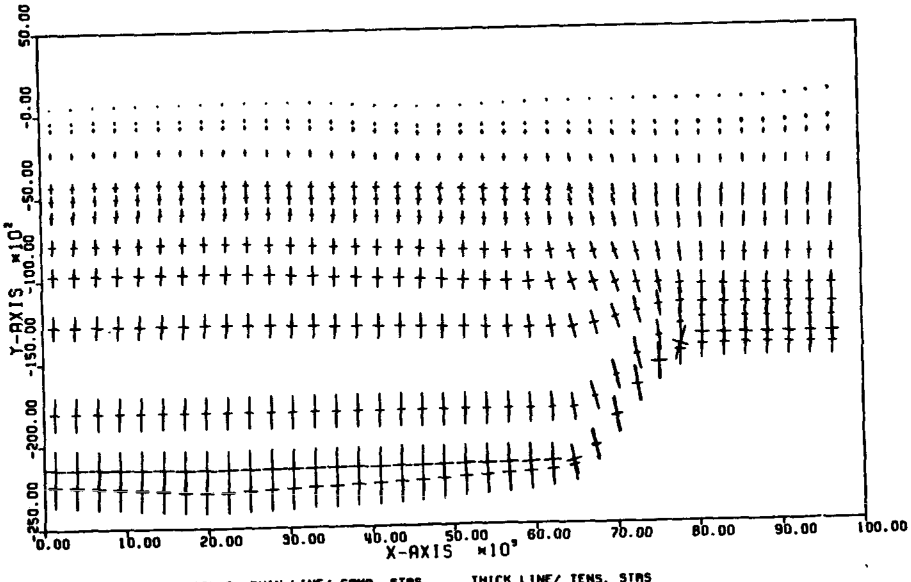

Fig. 4b—Principal stress plots for gravitational load model.

SPE

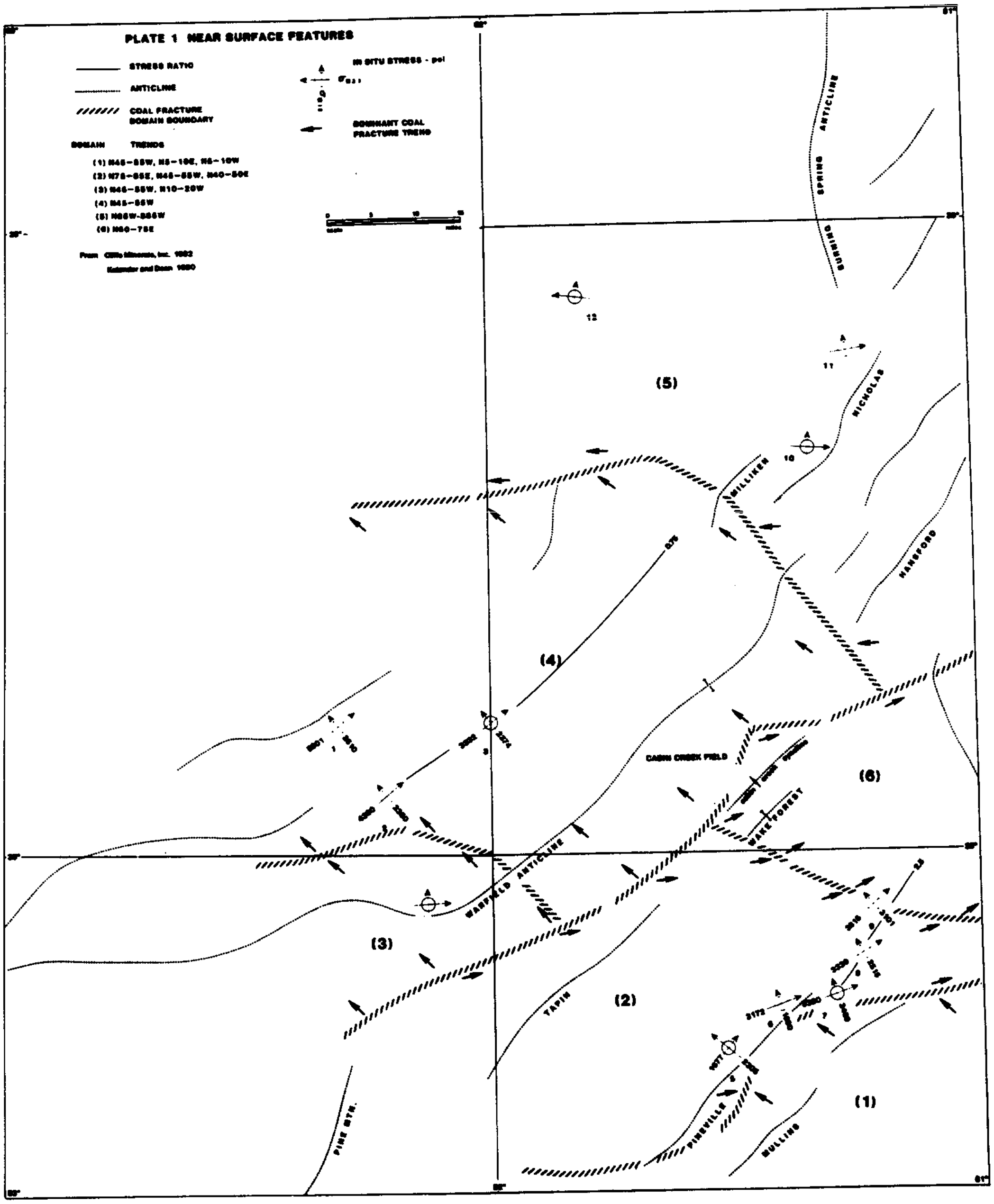

Fig. 5—Near surface tectonic features for region surrounding Cabin Creek field.

SPE 12860

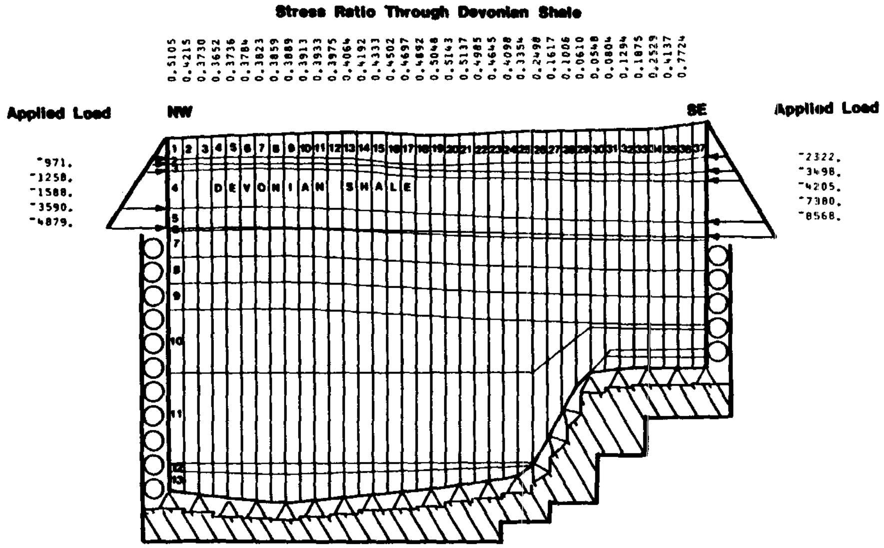

Fig. 6a—Tectonic load model with prescribed stress ratios at NW and SE boundaries.

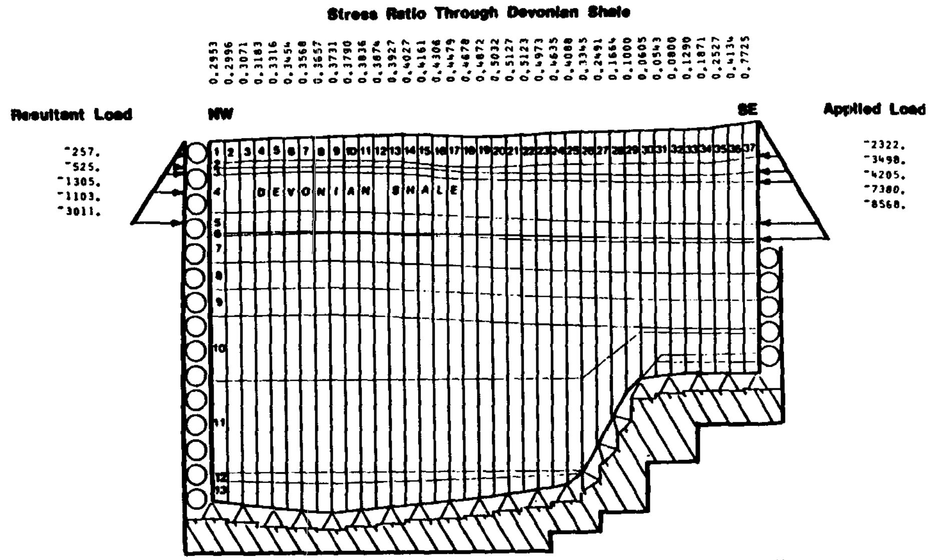

Fig. 7a—Tectonic load model with prescribed stress ratio at SE and confinement at NW.

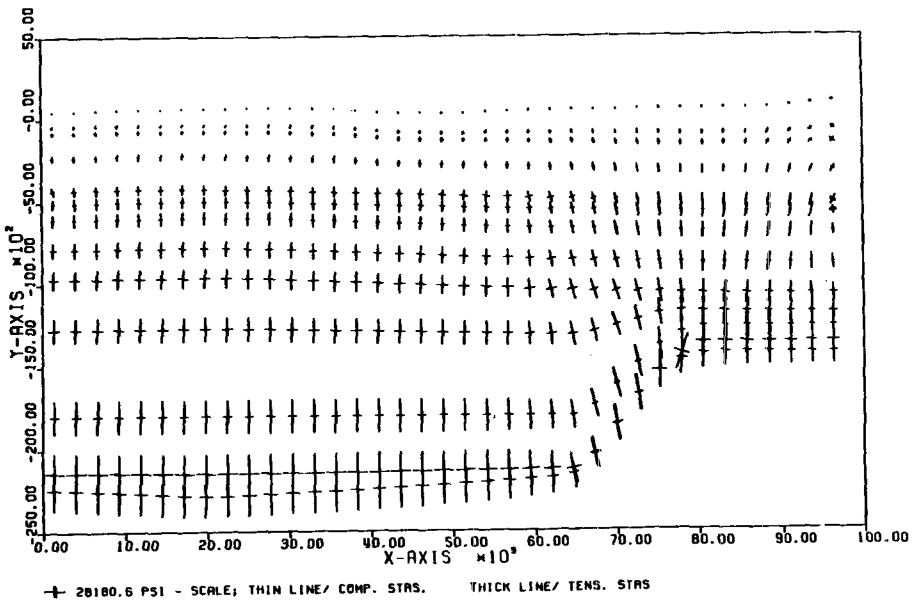

Fig. 6b—Principal stress plots for tectonic load model in Fig. 6a.

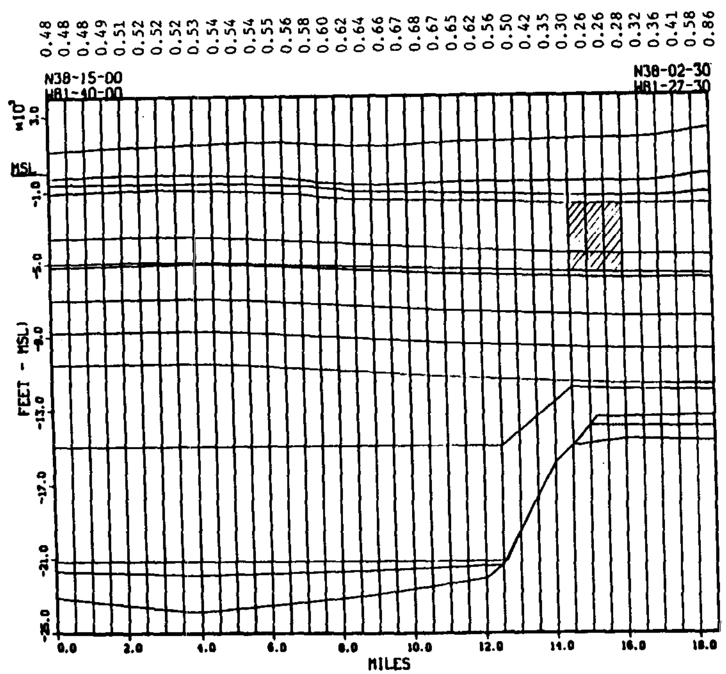

Fig. 7b—Stress ratios for tectonic load model with K = 1 at SE, confinement at NW, and reduced elastic model in Unit 6. Hatched zones indicate failure regions.

SPE 1286